Water Resour Manage (2012) 26:3267–3283
DOI 10.1007/s11269-012-0071-8

Aerodynamic Parameterization of the Satellite-Based Energy Balance (METRIC) Model for ET Estimation in Rainfed Olive Orchards of Andalusia, Spain

C. Santos · I. J. Lorite · R. G. Allen · M. Tasumi

Received: 29 March 2011 / Accepted: 17 May 2012 /
Published online: 6 June 2012

Abstract Sensitivity of estimates of evapotranspiration (ET) for olive fields located in Andalusia (Spain) to aerodynamic parameterization in METRIC (*Mapping Evapo-Transpiration with high Resolution and Internalized Calibration*) was evaluated to better understand behavior of the model and spatial and temporal distribution of ET from olives, with the ultimate aim of designing customized irrigation schedules. Previous METRIC analyses have primarily focused on the estimation of ET over fields of annual crops, with few applications to complex canopies such as olive. The model was compared against FAO 56-soil water balance-based ET estimations for non-irrigated olive fields. In the first comparisons METRIC model used a general equation for momentum roughness length (z_{om}) based on a fixed function of height estimated from LAI (Leaf Area Index) that underestimated the olives height and therefore z_{om}, so that ET derived as a residual of the energy balance was over-estimated (RMSE=1.12 mm/day) compared to the soil water balance derived ET. The Perrier roughness function based on LAI and tree canopy architecture for sparse trees, coupled with improved olive height estimates (employing tree density and canopy shape factors) improved estimates for z_{om}. This approach produced closer comparisons to rainfall-constrained ET estimates based on soil water balance for rainfed olive orchards (RMSE=0.25 mm/day). This study does not attempt to validate METRIC results; instead utilizes a comparative approach between two independent methodologies to improve olive ET estimation via remote sensing, with the strong advantage, over the soil water balance approach, of improved spatial resolution over large areas.

C. Santos · I. J. Lorite (✉)
IFAPA, Centro "Alameda del Obispo", Alameda del Obispo s/n, Post office box: 3092, 14080 Córdoba, Spain
e-mail: ignacioj.lorite@juntadeandalucia.es

R. G. Allen
Water Resources Engineering, University of Idaho, 3793 N. 3600 E., Kimberly, ID 83341, USA

M. Tasumi
Faculty of Agriculture, University of Miyazaki, Miyazaki 889-2192, Japan

Keywords Rainfed olive · Evapotranspiration · FAO 56 model · METRIC · Momentum roughness length · Perrier function · Soil water balance

1 Introduction

Olive orchards are one of the most important crops in the semiarid Mediterranean region. Olives covered about 4.3 million of ha in Europe in 2007, of which 50 % were located in Spain (Eurostat 2011). Traditional olive orchards in Spain are rainfed, with around 100 trees per ha and ground cover rarely exceeding 25 % and generally located on hillsides.

Crop-water requirements for olive vary during the growing period and among orchards, mainly due to variation in crop canopy and density and in climatic conditions. Scientific efforts in measuring evapotranspiration of olive orchards are all relatively recent (Testi et al. 2004). A common method for assessing olive ET is the direct measurement of the total water vapour flux density from the orchard using the eddy covariance technique (Villalobos et al. 2000; Testi et al. 2004; Martínez-Cob and Faci 2010). However, these methods generally sample ET from single orchards or parts of orchards, only. Whole orchard ET has been measured in olive using the water balance method (Michelakis et al. 1996; Palomo et al. 2000) and estimated using daily soil water balance – atmospheric process models such as the relatively simple FAO 56 model which is based on the concepts of reference evapotranspiration ET_o, crop coefficient K_c and root zone water balance (Allen et al. 1998). The K_c ET_o approach has been commonly used for the estimation of olive water requirements in commercial orchards, and also to understand the relations between water use and yield (Martín-Vertedor et al. 2011). Er-Raki et al. (2010) have evaluated the ability of the FAO 56 dual crop coefficient model to reproduce the temporal evolution of ET and its components in olive. However, there is no simple way to calculate crop coefficients for olives, as they must integrate several factors depending on agricultural practices and orchard architecture (Er-Raki et al. 2008; Allen and Pereira 2009; Minacapilli et al. 2009; Cammalleri et al. 2010a; b). Allen and Pereira (2009) provided an updated formulation for estimating potential K_c for orchards as a function of fraction of ground shaded by the canopy and climate.

Remote sensing techniques represent a promising tool to overcome problems related to uncertainties in crop coefficient calculation in olive and other crops having sparse woody canopies, as suggested by studies carried out by Er-Raki et al. (2008) for an olive orchard in Central Morocco and by Hoedjes et al. (2008) who used an eddy covariance system to compare against daily ET values derived using ASTER satellite-based instantaneous estimates of ET from an olive orchard. Compared with traditional K_c-based ET estimations in olive orchards, remote sensing methods have a strong advantage in spatial accuracy because of the estimation ET by energy balance for each pixel of a satellite image using observed reflected radiation and temperature. Therefore, characterization of individual fields, including impacts of canopy density and tree spacing as well as relative water supply, are better addressed.

Surface energy balance (SEB) approaches for direct estimation of actual evapotranspiration have been developed over the past 20 years (Norman et al. 1995; Roerink et al. 1997; Bastiaanssen et al. 1998; Kustas and Norman 1999; Allen et al. 2007a; Gontia and Tiwari 2010; Awan et al. 2011; Elhag et al. 2011). These approaches have recently been applied to estimate ET from a variety of sparse woody canopies, for example, by Samani et al. (2009) to estimate the daily ET for pecan orchards in the lower Rio Grande Valley, New Mexico. The SEBAL model has been tested over grapes, peaches and almonds in Spain, Turkey and

California (Bastiaanssen et al. 2008). Minacapilli et al. (2009) compared two SEB approaches, the SEBAL model and the TSEB (Two-Source Energy Balance model; Norman et al. 1995) to estimate the actual ET from typical spatially sparse Mediterranean vegetation (with olive, citrus and vineyards). However, this analysis did not determine which SEB model produced better performance. Cammalleri et al. (2010a) applied a coupled hydrological/SEB model to estimate actual evapotranspiration in an irrigated olive grove from a semi-arid region located in Sicily. The model was compared with energy fluxes measurements from a dual-beam small aperture scintillometer system.

METRIC (*Mapping EvapoTranspiration with high Resolution and Internalized Calibration*) is a blended-source energy balance-based ET estimation model developed by the University of Idaho, USA (Allen et al. 2007a) and originated from the SEBAL model of Bastiaanssen et al. (1998). METRIC has been applied in the Western United States (Allen et al. 2005, 2007b) and in Southern Spain (Santos et al. 2008, 2010), to produce high resolution ET maps from the Landsat satellite. Estimates of ET by METRIC have compared favourably with a series of lysimeter ET measurements at two locations in the Northwest US (Tasumi et al. 2005) and with measured fluxes via eddy covariance in central Iowa (Choi et al. 2009). However, there has not been extensive testing nor focused application on non homogeneous or sparse woody canopies, such as olives, where biases in model estimates may be caused by the soil and shadow effects on pixel temperature estimation and uncertainties regarding roughness and aerodynamic profiles, mixture and shading effects on surface temperature (T_s) and the near surface air temperature gradient (dT) function in the sensible heat flux calculation (Allen et al. 2007a).

The procedure used in METRIC, where a single dT function and aerodynamic resistance (r_{ah}) term are used to estimate H, is referred to as a blended model (Allen et al. 2011), where the lower endpoint of dT and r_{ah} are placed in the equilibrium boundary layer at some z_1 distance above the zero plane displacement height. The intention is to estimate the near surface temperature gradient and aerodynamic conductance in the mixed, somewhat chaotic layer of air where dT and r_{ah} combine effects of both vegetation and soil surface. This approach seems justified, especially under conditions of greater than calm wind speed, where horizontal flow of air from vegetation to soil and from soil to vegetation is poorly structured and includes the combination with more vertical aerodynamic structures created by buoyancy for differentially heated surfaces (sunlit soil vs. shaded soil and sunlit, dry canopy vs. shaded canopy). The large spatial size of thermal pixels in Landsat images (60–120 m) produces blended, bulk values for T_s that tend to correlate with the blended dT, producing ET as a residual of the energy balance for sparse olive orchards that are in line with independent estimates, as shown for this study. The use of the blended layer model reduces speculation or potential component malformation in TSEB models associated with the largely unknown and canopy architecture-specific microscale air circulations and feedbacks between soil and canopy that are, in turn, associated with differential heating, air bouyancies, and mechanical forcings. Although the TSEB model might be more suitable for sparse canopies, uncertainties in parameterizing the intercanopy processes noted above were judged to create too much uncertainty in model behavior and too much 'freedom' in model parameterization. The application and calibration of a TSEB model in this study would have been complicated for the relatively large number of fields and canopy architectures in the study. The calibration of the blended layer METRIC model uses upper and lower ranges of radiometric temperature and fractional vegetation cover within a scene to internally calibrate its variables and to remove many systematic biases in satellite retrievals and assumptions regarding energy balance components (Allen et al. 2011). TSEB generally uses the remotely sensed data as direct inputs to the computation of the soil, canopy aerodynamic surface temperatures and heat flux components. As result, TSEB has greater sensitivity to uncertainty in radiometric temperature values caused by error in atmospheric and emissivity corrections and to error or uncertainties in defining the spatially distributed air temperature that can vary widely with partitioning of available energy. Air temperature is implicitly tied to dT in the blended METRIC approach.

The objective of this work was to contrast METRIC results for olives made for year 2005 against water balance-based ET estimations from non-irrigated olive fields where ET was constrained by rainfall data and stored soil moisture. Similarity in estimates by the methods reveals strengths of each method regarding accuracy of simulation and parameterizations and sensitivity to how components are estimated. Differences in estimates indicate where behaviour of SEB or soil water balance models is not well understood or where models are inadequately defined and where more work is needed.

2 Materials and Methods

2.1 Selection of Fields for ET Evaluation

Sixty-seven non-irrigated olive fields in the eastern portion of Córdoba province were investigated during the evaluation of METRIC. The ET from these olive fields was estimated using the FAO 56 K_c ET_o/soil water balance-based method (Allen et al. 1998) and using the METRIC model. For both methodologies, weather data including rainfall, air temperature, relative humidity, wind speed and solar radiation from five weather stations within or near the study area were obtained from the Agroclimatic Information Network of Andalusia (Gavilán et al. 2006). METRIC was applied to Landsat 5 satellite images for the period between 22 April and 13 September, 2005. In sampling METRIC-based ET, 30 sample pixels were identified and selected per field where all sampled pixels resided at least 120 m inside field boundaries to avoid the contamination of thermal pixels of the Landsat 5 satellite by areas lying outside the fields. Small fields that did not meet these requirements were eliminated from the selection, so that finally 22 non-irrigated olive fields with an averaged size of 72 ha qualified for the study (Fig. 1). Average tree density on these fields ranged from 70 to 200 trees per ha, and ages of trees ranged from approximately 20 to 50 years. Tree heights ranged from 1.7 to 6 m across the fields.

2.2 Water Balance-Based Estimates

ET from the non-irrigated olive fields was estimated using the FAO 56 dual K_c based daily soil water balance method (Allen et al. 1998):

$$ET_{c(adj)} = (K_s K_{cb} + K_e) ET_o \tag{1}$$

where K_s is a water stress coefficient, K_{cb} is the basal crop coefficient, K_e is the soil evaporation coefficient, and ET_o is grass reference evapotranspiration. The water stress coefficient is obtained following Allen et al. (1998) as:

$$K_s = \frac{TAW - D_r}{(1 - p) \cdot TAW} \tag{2}$$

where TAW is the total available soil water in the root zone (mm), D_r is the root zone

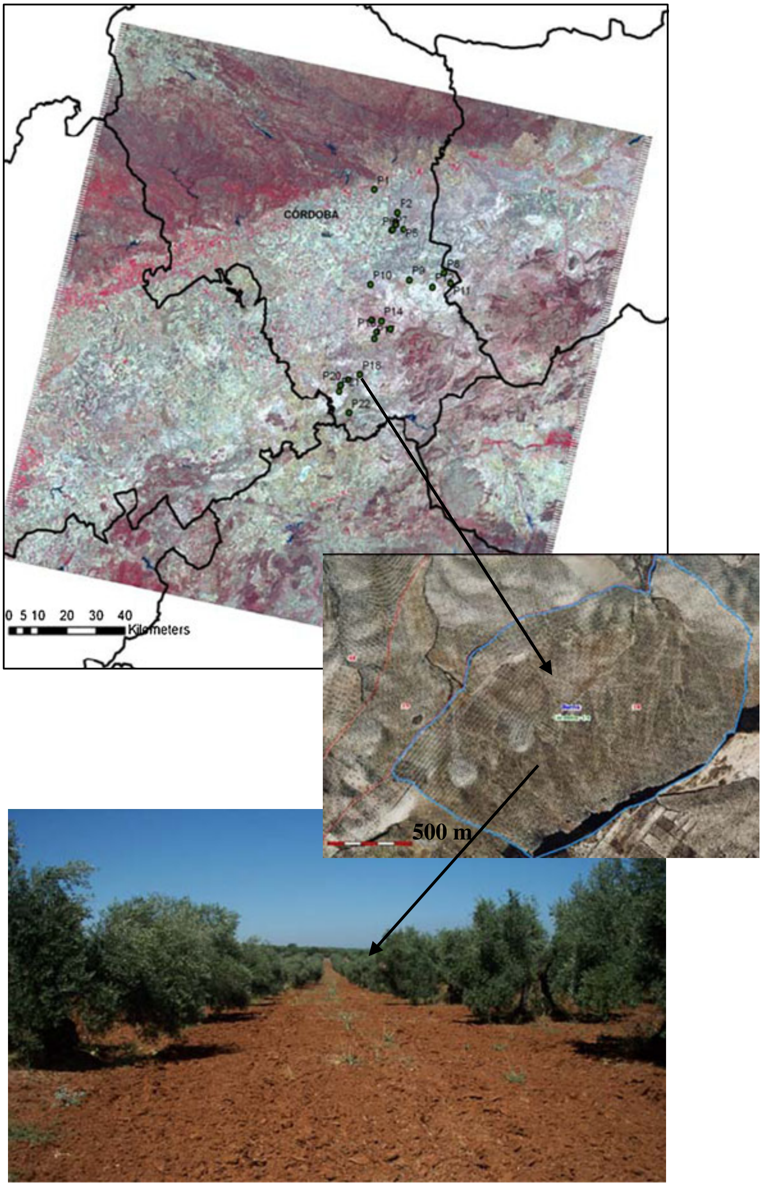

Fig. 1 Selected non-irrigated olive fields located east/south of Córdoba, Spain, aerial photograph and detail of one of these fields, overlaid on a Landsat 5 image

depletion (mm) and p is the fraction of TAW that a crop can extract from the root zone without suffering water stress. The primary soil type in the study area was silt loam, estimated to hold 150 mm/m of available water. The root zone of the rainfed olives was set at 1.5 m depth based on typical rooting by olives (Allen et al. 1998), and p was set at 0.65 for the olive crop, following Allen et al. (1998). The root zones were assumed to be dry at the beginning of the simulation period (September 1, 2004), which followed a very dry summer.

Estimates for K_{cb} were based on average groundcover and tree height of the sampled fields, and adjusted for climate and reduction for effective stomatal control on transpiration following Allen et al. (1998) and Allen and Pereira (2009). First we obtained a $K_{cb\ mid}$ from an effective ground cover of 0.25 and height of 4 m where a reduction factor for stomatal control was set to 0.67 (Allen et al. 1998, p 192), and adjustment was made for impacts of the dry, windy climate of the study area where wind speed at 2 m averages 2.2 m/s and average daily minimum RH averages 19 % during the summer. The resulting value obtained for $K_{cb\ mid\ adj}$ was 0.5, based on a value for the ML coefficient of Allen and Pereira (2009) of 1.8, and the values of $K_{cb\ ini\ adj}$ and $K_{cb\ end\ adj}$ were set to 0.42, to maintain proportions to baseline K_{cb} values from Allen and Pereira (2009) of 0.3, 0.35 and 0.3 for the same effective fraction of ground cover and a standard climate.

Er-Raki et al. (2010) obtained an average seasonal value of basal crop coefficient of 0.54 in a Moroccan olive orchard having similar semi-arid conditions using sap flow measurements. That value is similar to our K_{cb} values. The K_e coefficient was estimated using potential values for K_c, a soil evaporation reduction coefficient K_r, and the exposed and wetted soil fraction (0.75).

Results of the FAO 56 soil water balance-based (SWB) calculations are summarized in Fig. 2 and Table 1. The 2005 season was extremely dry, and the FAO 56 model and water balance estimated large amounts of water stress for the non-irrigated olive trees, so that the K_s function tended to dominate over the K_{cb} and K_e estimates. The model suggested that essentially all rainfall during the 12 month period was evaporated or transpired, with no gain in soil water storage nor any deep percolation flux to ground-water over the 12 month period. The time series of ET shown in Fig. 2 was created using rainfall, ET_o, soil type and tree architecture data averaged over the 22 fields. The spikes in ET during May and September were caused by evaporation stemming from rain events. Extremely low ET_c values were detected during July and August due to extremely dry conditions (see Table 1). As a confirmation of the extreme dryness, trees were observed to lose leaves during this period. The similarity of results from all five weather stations permitted the comparisons with METRIC and statistical analyses to be based on averages over the stations.

2.3 Improving METRIC ET Application for Olives

2.3.1 Standard METRIC z_{om} Estimate

The METRIC energy balance procedure (including the Mountain model) of Allen et al. (2007a) was applied to seven Landsat 5 images spread across the 2005 growing season. METRIC-based ET was produced as a residual of the surface energy balance, where energy consumed by the ET process was calculated as a residual of the surface energy equation:

$$LE = R_n - G - H \tag{3}$$

where LE is the latent energy consumed by ET, R_n is net radiation, G is sensible heat flux conducted into the ground, and H is sensible heat flux to the air.

Net radiation was computed by subtracting all outgoing radiant fluxes from all incoming radiant fluxes and included solar and thermal radiation, considering the slope effects on the solar components of the energy balance. Soil heat flux was estimated as a function of net radiation, vegetation indexes and surface temperature (T_s), where surface temperature is computed using the Landsat satellite thermal sensor. Sensible heat flux was estimated by deriving a near surface air-temperature gradient (dT) and aerodynamic resistance between

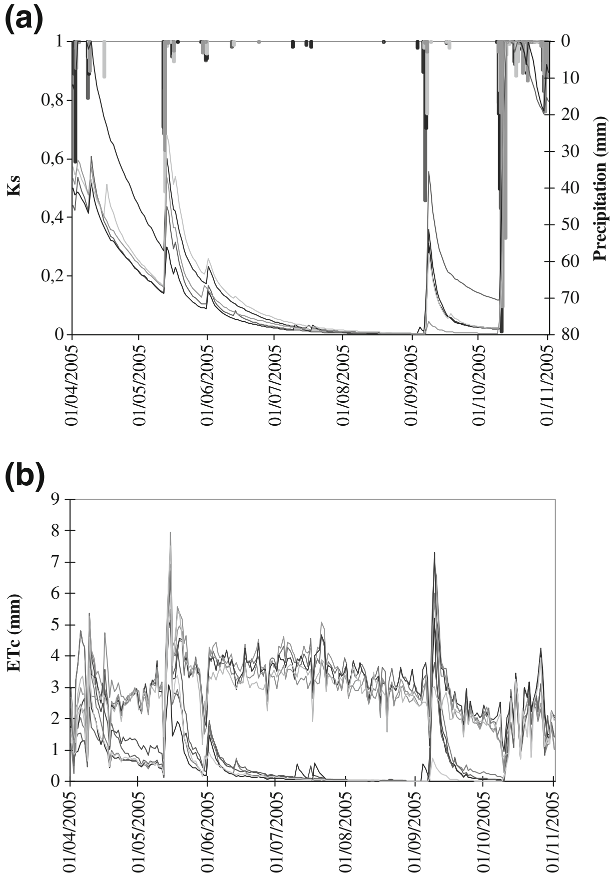

Fig. 2 **a**) Water stress coefficient (K_s) and precipitation for each of five weather stations used in the study; **b**) SWB-derived potential and adjusted evapotranspiration for the five weather stations used in the study data

two near surface heights (0.1 and 2 m above the zero plane displacement), and assuming dT in the blended layer to be linear in proportion to radiometric T_s. This approach constitutes one of the pioneering components of the SEBAL model developed by Bastiaanssen (1995), who provided empirical evidence for using the linear relation between dT and T_s. Calibration

Table 1 Annual rainfall amounts and ET_o (mm) for the September 2004 to September 2005 period and associated estimated ET from non-irrigated water-stressed olives by the FAO 56-based dual K_c and soil water balance method for the five weather stations used in the study

Station	El Carpio	Córdoba	Santaella	Marmolejo	Lora de Río
Latitude	37°54′54″N	37°51′42″N	37° 31′25″N	38° 03′26″N	37° 39′37″N
Longitude	04°30′09″W	04°48′00″W	04°53′03″W	04°07′46″W	05° 32′ 19″ W
Elevation (m)	165	117	207	208	68
Rainfall (mm)	309	365	271	321	273
ET_o (mm)	1632	1582	1650	1472	1521
$ET_{SEASONAL}$ (mm)	303	366	271	323	276

of the dT function was accomplished by selecting two extreme "calibration pixels" representing very dry and very wet agricultural surfaces, as described in Allen et al. (2007a). Daily ET, ET_{24} was estimated by assuming that the instantaneous ET_rF (ratio between current and reference ET) computed at image time was the same as the average ET_rF over the 24 h average. This assumption has been validated through lysimeter measurements as shown in Allen et al. (2007a, b).

METRIC-estimated ET was used to describe the degree of water stress over time by computing a METRIC water stress coefficient ($K_{s\,METRIC}$), that is similar to, and was compared against, the FAO 56 water stress coefficient:

$$K_{s\,\mathrm{METRIC}} = \frac{\mathrm{ET}_{\mathrm{METRIC}}}{\mathrm{K_{cb}} \cdot \mathrm{E\,T_o}} - \frac{\mathrm{K_e}}{\mathrm{K_{cb}}} \tag{4}$$

where K_{cb} and K_e were averaged values of the basal and evaporation coefficient from the FAO-56 SWB model, with K_{cb} representing potential (non-stressed) conditions. The inclusion of K_e in Eq. 4 is necessary because the ET_{METRIC} estimate contains a soil water evaporation component.

The initial applications of METRIC used a general equation for momentum roughness length (z_{om}) that is designed for annual agricultural crops and conditions (Allen et al. 2007a):

$$z_{om} = 0.12h \tag{5}$$

where z_{om} is in meters, h is crop height (m). Roughness length is used to estimate momentum transport, which is a measure of the form drag, air turbulence and skin friction for the layer of air that interacts with the surface. This is used in METRIC in the aerodynamic resistance-based estimation of sensible heat flux (Allen et al. 2007a). In general, the smaller the value specified for z_{om} in METRIC, the smaller the estimate for sensible heat flux, and thus the larger the estimate for ET calculated as a residual of the energy balance.

The initial estimate for h was based on a standard METRIC algorithm by Tasumi (2003) for annual, irrigated crops characteristic of the temperate climate of Kimberly, Idaho, USA, and is based on estimated LAI (Leaf Area Index):

$$h = 0.15\mathrm{LAI} \tag{6}$$

In the case of olives, h is substantially underestimated by Eq. (6), and therefore, z_{om} is underestimated, so that ET is overestimated. Application of Eqs. 5 and 6, developed for dense, annual crops, is inappropriate for sparse olive orchards, but was included to demonstrate sensitivity of METRIC ET estimation to error in z_{om} for a stressed, rainfed system.

2.3.2 Estimating z_{om} Using Olive Height and Tree Density

Orgaz et al. (2005) defined a *Shape Index* to describe the canopy architecture of olive trees as the ratio between the olive crown diameter and height. The ratio tends to vary with density of olive plants for old Spanish orchards (Table 2) and was used here to estimate z_{om}, where crown diameters were estimated using 0.5 m ortho-rectified aerial imagery collected over the entire area of the study (Junta de Andalucía 2002). Olive tree density was estimated by counting and identifying the center point of each tree, resulting in an image with 1x1m pixels assigned a digital number of "1" if an olive tree and "0" otherwise. That image was aggregated to produce a coarsened density map having 30 m resolution by multiplying all pixels by 900 and then, using a degradation tool, calculating the average value. The resulting map expressed the number of trees per 30x30m pixel. Olive tree height was estimated using the crown density and Shape Indices previously determined (Table 2). The estimates of tree height averaged 4.4 m, which is much more realistic than the value of 0.03 m that resulted from Eq. 6, due to the low LAI of olive trees. Finally values for z_{om} were estimated from h using Eq. 5.

2.3.3 The Perrier Function for z_{om}

Perrier (1982) developed a z_{om} function based on LAI and tree canopy architecture for sparse trees:

$$z_{om} = \left(\left(1 - \exp\left(\frac{-aLAI}{2}\right)\right)\exp\left(\frac{-aLAI}{2}\right)\right)h \tag{7}$$

where a is an adjustment factor for the LAI distribution within the canopy with a=(2f) for $f\geq$ 0.5 and a = $(2 \cdot (1 - f))^{-1}$ for f<0.5. The factor f is the proportion of LAI lying above h/2. In the case of the olives of the study, they are mostly old trees, where nearly 40 % of branches lay above the half-way point (f=0.4), so an appropiate value for a is 0.83. Various other models such as those by Raupach (1992, 1994, 1995) have been proposed to describe z_{om} for sparse canopies, but those models contain a number of coefficients whose values must be determined empirically. The Perrier function performs similarly to the Raupach density-based functions.

LAI values were computed in the METRIC procedure using the soil adjusted vegetation index (SAVI; Allen et al. 2007a) as:

$$LAI = -\frac{\ln[(0.69 - SAVI)/0.59]}{0.91} \tag{8}$$

where, for application with Landsat images, SAVI is based on top of atmosphere reflectance of bands 3 and 4 and the SAVI parameter "L" was set to 0.1.

Low LAI values are common to traditional rainfed orchards, where representative LAI for 30 % ground cover is about 0.33 (Gómez et al. 2001). Our values were even lower in some cases, as our ground cover was also lower, with maximum LAI for olive orchards in the study of around 0.4 and decreasing from April to July due to intense pruning and due to a decrease in green vegetation beneath trees that dried up during summer. In addition there was some reduction in numbers of leaves of olives resulting from stress during the summer period. The average Perrier multiplier from Eq. 7, averaged over the 22 fields and seven

Table 2 Values of the *Shape Index* (SI = D/H) for old olive orchards in Spain having different plant densities (following Orgaz et al. 2005) where D is crown diameter and H is tree height, both in meters

Density (olives/ha)	D/H
Less than 55	1.50–1.60
60–90	1.40–1.45
100–125	1.30–1.35
130–170	1.20–1.25
175–230	1.10–1.15
240–275	1.00–1.05
280–350	0.90–0.95
more than 360	0.80

Landsat images, produced an average z_{om}/h relationship:

$$z_{om} = 0.068h \quad (9)$$

3 Results

3.1 Application of the Standard METRIC z_{om} Estimate

Crop coefficients K_{co} derived for the 22 non-irrigated sample fields from METRIC are plotted in association with the continuously modelled averaged K_{co} from the SWB model in Figs. 3a. These plots suggest some over-estimation of ET by the initial application of METRIC using the standard *h* vs. LAI relationship of METRIC for the non-irrigated olive orchards (RMSE of K_{co}=0.188 and of ET=1.12 mm/day). However, the midsummer depression of ET from the rainfed olive fields was in relatively good agreement with the ET as modelled by the SWB due to the large magnitude of stress reduction to K_c during this period as determined by low available soil water, which is in turn, governed by precipitation, which is considered to be known with relatively good accuracy. The variation in METRIC-derived K_{co} among the 22 fields was caused by variation in size of tree canopy, tree age, style of tree pruning, soil type and depth, and also to some degree, random error in the K_{co} estimated by METRIC stemming from minor variation in surface temperature for the same energy balance condition.

Figure 3a shows METRIC results for K_{co} using z_{om} based on Eq. 5 combined with an improved estimate for *h* from the D/H ratios of Orgaz et al. (2005). This method for z_{om} caused, on average, some underestimation of ET in comparison to the SWB estimates for 3–4 images during mid-spring and summer although comparisons were good for other dates (RMSE of K_{co}=0.058 and of ET=0.34 mm/day). Figure 3b compares the SWB-estimated water stress coefficient (K_s) and a METRIC-derived K_s from Eq. 4 for the z_{om}/h=0.12 estimation. Because the z_{om}/h relationship of Eq. 5 is based on a dense vegetation cover, this relationship does not apply well to olive trees having only partial ground cover.

3.2 z_{om} Derived from the Perrier Function

The z_{om} function developed by Perrier (1982) for tall and potentially sparse vegetation such as forests, riparian areas or orchards was applied in METRIC calculations, where z_{om} was calculated from z_{om}/h=0.068. That approach produced estimates for K_{co} that were closest to the SWB-based estimates (RMSE of K_{co}=0.045 and of ET=0.25 mm/day; Fig. 4a). Figure 4b shows METRIC-derived water stress coefficients using the Perrier function compared with SWB-based estimates. The similarity and consistency of estimates by the METRIC energy balance and by the FAO 56 dual K_c and water balance model is quite good. There was some disagreement for the last METRIC image (13/09/05), where SWB-based estimates, averaged over the five weather stations, did not incorporate effects of spatial variability in precipitation (see Fig. 2).

The similarity of estimates between models does not validate either model, since validation via measurement of ET from the 22 rainfed fields examined in this study was logistically not possible. However, the FAO based estimates for ET were constrained by reported rainfall data, so that, integrated over time, the estimates are considered to be accurate and largely independent of METRIC.

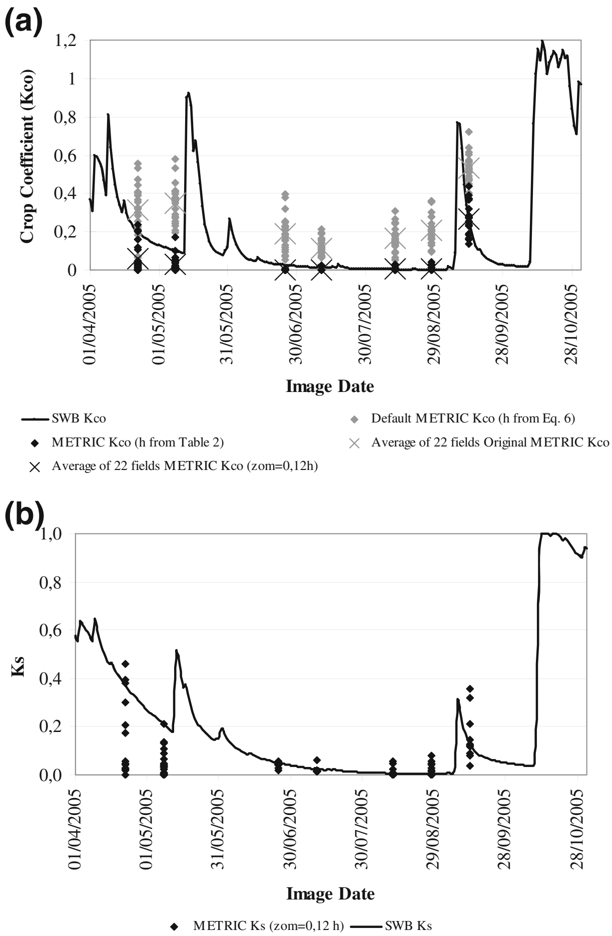

Fig. 3 **a**) K_{co} derived from METRIC formulation using *h* from equation 6 and from Table 2 vs. results from the SWB model; **b**) METRIC water stress coefficients (K_s) and SWB-based estimates of ET for actual conditions

3.3 Sensitivity Analyses on Soil Parameters and K_c

Sensitivity analyses were made to the SWB model to determine to extent to which ET and actual K_{co} derived from that model (via Eq. 1) vary with changes in values for soil parameters. Results are summarized on Table 3.

First we evaluated the influence of soil water storage at the beginning of the simulation period where we initially assumed that the initial soil condition was dry. Figure 5a shows SWB-derived water stress coefficients (K_s) and crop coefficients (K_{co}) averaged over the five weather stations for three different initial conditions (dry, 25 and 50 mm), starting at 1 September, 2004. Differences in K_{co} only occurred during the first 3–4 months, and were nearly zero by the time of the first METRIC image, in April, 2005, when all additional initial water had been extracted by the model. The computed RMSE between FAO-SWB-estimated K_{co} and METRIC determined K_{co} were very similar for the three initial conditions (Table 3).

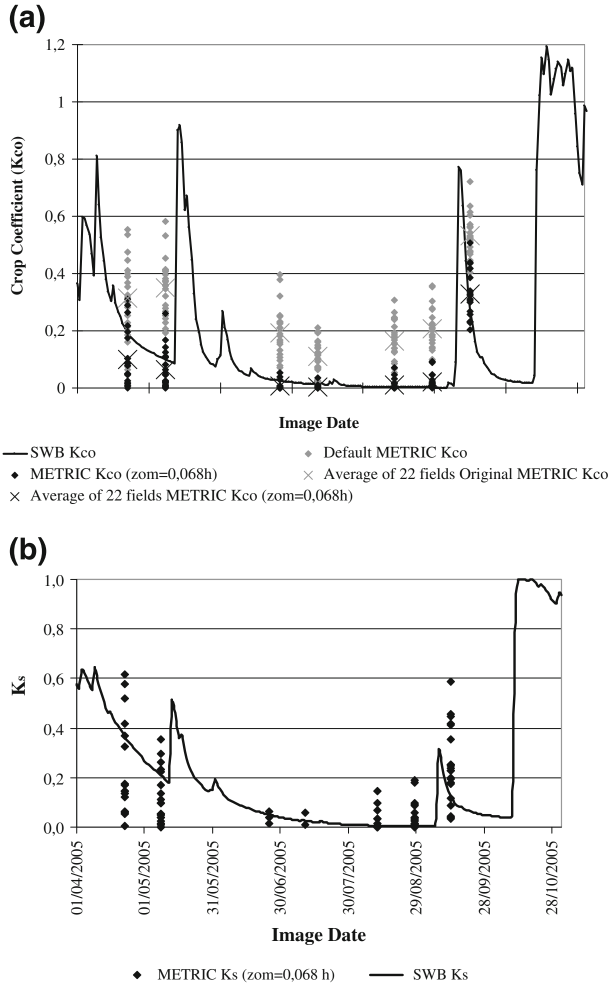

Fig. 4 **a**) K_{co} derived from default METRIC formulation and using z_{om}=0.068 h (where h is obtained from Table 2), vs. results from the SWB model; **b**) METRIC water stress coefficients (K_s) and SWB-based estimates of ET for actual conditions

A second sensitivity analysis was conducted on the influence of the depletion fraction (*p*) used to indicate the initiation of water stress on the K_c estimate from the SWB model. Figure 5b shows average SWB-based K_s and K_{co} averaged over the five weather stations for different values for *p,* where no important differences were found when compared with METRIC estimates. The relative insensitivity to *p* is expected, since, by midsummer, all available water was extracted, regardless of the value for *p*, and because K_s is so strongly influenced by total soil water holding capacity and rooting depth when time between wetting events is large.

A third sensitivity analysis was made on water holding capacity (WHC) and root zone depth (R_z), as these values impact the total water supply, and thus, control how low the value for K_s may become during summer (depending on water storage from winter; Table 3). However, insignificant change occurred in SWB-based K_s estimates when compared with

Table 3 Sensitivity analysis on the FAO 56 soil water balance model showing RMSE of K_{co} using tree height as determined from Table 2 (last 2 columns)

RMSE of K_{co}	Default METRIC z_{om} and h function	z_{om}=0.12 h	z_{om}=0.068 h
Actual conditions*	0.188	0.058	0.045
p=0. 55	0.182	0.066	0.054
p=0. 60	0.185	0.062	0.050
Initial soil water storage=25 mm	0.186	0.062	0.049
Initial soil water storage=50 mm	0.183	0.069	0.055
WHC=120 mm/m	0.201	0.063	0.053
WHC=160 mm/m	0.185	0.058	0.041
R_z=1 m	0.194	0.053	0.039
R_z=2 m	0.182	0.069	0.056
$K_{cb\ ini}$=0.3; $K_{cb\ mid}$=0.35; $K_{cb\ end}$=0.3	0.186	0.070	0.063
$K_{cb\ ini}$=0.46; $K_{cb\ mid}$=0.54; $K_{cb\ end}$=0.46	0.189	0.056	0.041

* Soil water storage at the beginning of the simulation period=0 mm; p=0.65; WHC=150 mm/m; R_z=1.5 m; K_{cb}=0.42, 0.5 and 0.42 for $K_{cb\ ini}$, $K_{cb\ mid}$ and $K_{cb\ end}$ respectively

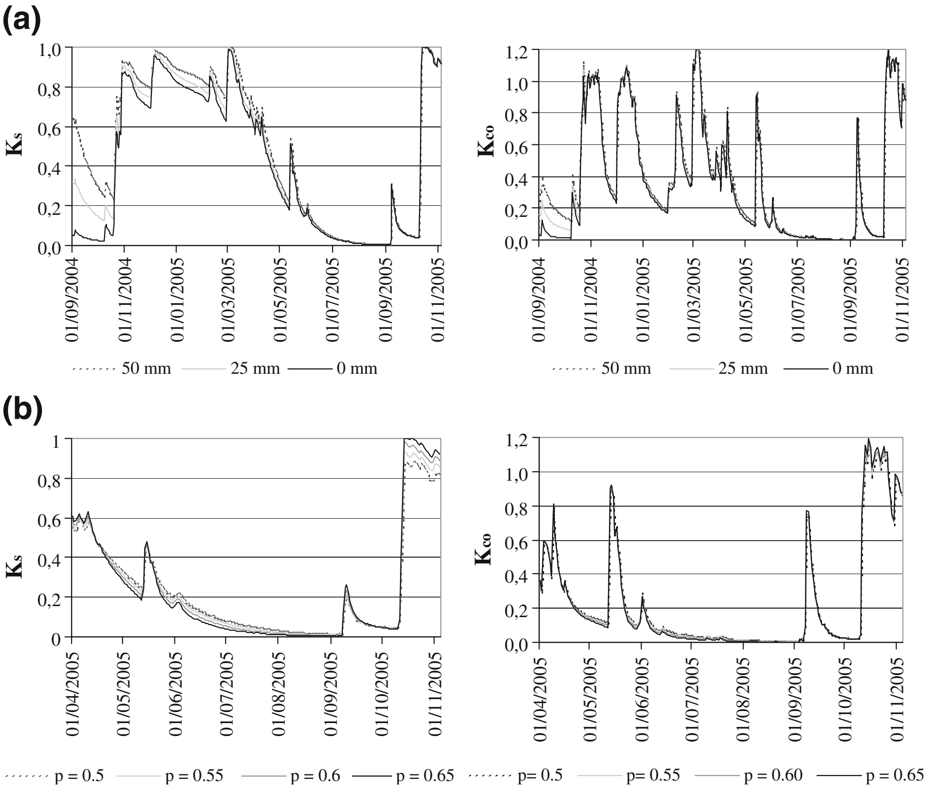

Fig. 5 **a**) SWB-based water stress coefficients and crop coefficients produced using different soil water contents at the beginning of the simulation period and **b**) different depletion fraction (p) values

METRIC estimates for the different WHC and root zone depth values, because total water in the root zone was constrained by precipitation input and initial available water.

The last sensitivity analysis examined the influence of K_{cb} (see Table 3) on soil water results and its agreement with METRIC estimates. Our initial values for K_{cb} were 0.42, 0.5 and 0.42 for $K_{cb\ ini}$, $K_{cb\ mid}$ and $K_{cb\ end}$ respectively. For the sensitivity analysis, we considered firstly 0.3, 0.35 and 0.3, as recommended by Allen and Pereira (2009) for a standard climate and then an average seasonal value for the basal crop coefficient of 0.54, based on sap flow measurements, obtained by Er-Raki et al. (2010) for similar semi-arid conditions. As expected, results were similar to those for the baseline conditions, as these changes only shifted the extraction of water in time, and soil water stress, via K_s, still dominated the process (data not shown in Figures).

The small differences produced by these sensitivity analysis showed that, due mainly to the scarce precipitation over the area during the 2005 study year, soil characteristics did not significantly influence the water balance-derived K_{co} estimates because rainfall inputs limited ET nearly all season, so that all likely values for soil parameters accommodated the storage and subsequent extraction of precipitation. Consequently the comparison of SWB-based results with METRIC estimations was considered to offer a relatively robust comparative basis for ET and K_{co}, which was the aim of this work.

4 Conclusions

Effective irrigation management and stress characterization in olive orchards requires an accurate methodology to quantify current evapotranspiration over large areas and at the spatial scale of individual orchards. Evapotranspiration from 22 non-irrigated olive fields under semi-arid conditions was assessed using the METRIC satellite-based energy balance model that until now had been mainly applied to agricultural fields having crops shorter and generally more dense than rainfed olives. The use of micrometeorological techniques was not feasible due to the large number of olive plots under study. Therefore, this study did not attempt to validate METRIC results using direct measurements of ET, but instead utilized a comparative approach between two independent models. The soil water balance model was based on the FAO 56 ET approach, where the crop coefficient (K_c) was estimated as a function of ground cover and height, a procedure that has been recently formalized in Allen and Pereira (2009). Some over-estimation of METRIC ET occurred for the non-irrigated olive orchards when crop height was estimated using a default METRIC algorithm intended for annual crops (RMSE=1.12 mm/day).

METRIC-based ET estimates for olives was improved using a methodology that tailored z_{om} estimation to the sparse tree crops by using a z_{om}/h ratio of 0.12, similar to that defined by Villalobos et al. (2000) and Berni et al. (2009) for intensive irrigated olive orchards, but with improved estimates for tree height (RMSE=0.34 mm/day). In our case this caused some underestimation of ET in comparison to the SWB-based estimates in the mid-spring and summer images due to the sparseness of our rainfed olives. On these dates the thermal signal of sparse olives was dominated by soil temperature and the large roughness value, and may have overstated sensible heat flux, and consequently the ET was underestimated. An alternative z_{om} function developed by Perrier (1982) for tall and sparse vegetation produced the most accurate estimate of K_{co} as compared with the SWB-based estimates (RMSE= 0.25 mm/day).

This study provides a useful indication of the impact of estimation procedure for crop height and z_{om} on aerodynamic behaviour of METRIC computations in application to sparse woody canopies. Results indicate that, with good estimates of z_{om}, ET estimated by METRIC compares well with modelled ET under water shortage-induced stress of rainfed olives. This supports the value of continued study on the use of METRIC or similar models to monitor ET behaviour of olive orchards in Southern Europe for the design of customized irrigation schedules and means to take strong advantage of the spatial information and relatively good accuracy of satellite-based products. Particularly in large olive areas of Andalusia, this approach constitutes a useful tool for Irrigation Advisory Services to achieve an efficient use of irrigation water especially during drought periods, in contrast with the traditional fixed schedules based on average data that are commonly used (Lorite et al. 2012). Furthermore, the determination of ET via remote sensing techniques can help identify water stress in olive orchards, and can be useful to analyze deficit irrigation strategies.

Acknowledgements The study was supported by grant AGR-6126 of the Regional Government of Andalusia. Development of the METRIC processing algorithms was supported by funding from the Idaho Agricultural Experiment Station, Idaho Department of Water Resources, the US Geological Survey, NASA, the National Science Foundation EPSCoR program EPS-0814387, and Raytheon Company.

References

Allen RG, Pereira LS (2009) Estimating crop coefficients from fraction of ground cover and height. Irrig Sci 28:17–34

Allen RG, Pereira LS, Raes D, Smith M (1998) Crop evapotranspiration: guidelines for computing crop water requirements. FAO Irrigation and Drainage Paper 56. FAO. Rome (Italy)

Allen RG, Tasumi M, Morse A, Trezza R (2005) A landsat-based energy balance and evapotranspiration model in western US water rights regulation and planning. Irrig Drain Syst 19:251–268

Allen RG, Tasumi M, Trezza R (2007a) Satellite-based energy balance for mapping evapotranspiration with internalized calibration (METRIC) - Model. J Irrig Drain Eng ASCE 133(4):380–394

Allen RG, Tasumi M, Morse A, Trezza R, Wright JL, Bastiaanssen W, Kramber W, Lorite IJ, Robison CW (2007b) Satellite-based energy balance for mapping evapotranspiration with internalized calibration (METRIC) – Applications. J Irrig Drain Eng ASCE 133(4):395–406

Allen RG, Irmak A, Trezza R, Hendrickx J, Bastiaanssen W, Kjaesgaard J (2011) Satellite based ET estimation in agriculture using SEBAL and METRIC. J Hydrolog Process 25:4011–4027

Awan UK, Tischbein B, Conrad C, Martius C, Hafeez M (2011) Remote sensing and hydrological measurements for irrigation performance assessments in a water user association in the Lower Amu Darya River Basin. Water Resour Manag 25:2467–2485

Bastiaanssen WGM (1995) Regionalization of surface flux densities and moisture indicators in composite terrain: A remote sensing approach under clear skies in Mediterranean climates. Ph.D. Dissertation, CIP Data Koninklijke Bibliotheek, Den Haag, The Netherlands

Bastiaanssen WGM, Menenti M, Feddes RA, Holtslag AAM (1998) A remote sensing surface energy balance algorithm for land (SEBAL): 1. Formulation. J Hydrol 212–213:198–212

Bastiaanssen WGM, Pelgrum H, Soppe RWO, Allen RG, Thoreson BP, de C Teixeira AH (2008) Thermal infrared technology for local and regional scale irrigation analysis in horticultural systems. ISHS Acta Hort 792:33–46

Berni JAJ, Zarco-Tejada PJ, Sepulcre-Cantó G, Fereres E, Villalobos F (2009) Mapping canopy conductance and CWSI in olive orchards using high resolution thermal remote sensing imagery. Remote Sens Environ 113:2380–2388

Cammalleri C, Agnese C, Ciraolo G, Minacapilli M, Provenzano G, Rallo G (2010a) Actual evapotranspiration assessment by means of a coupled energy/hydrologic balance model: validation over an olive grove by means of scintillometry and measurements of soil water contents. J Hydrol 392:70–82

Cammalleri C, Anderson MC, Ciraolo G, Durso G, Kustas WP, La Logia G, Minacapilli M (2010b) The impact of in-canopy wind profile formulations on heat flux estimation in an open orchard using the remote sensing-based two-source model. Hydrol Earth Syst Sci 14:2643–2659

Choi M, Kustas WP, Anderson MC, Allen RG, Li F, Kjaersgaard JH (2009) An intercomparison of three remote sensing-based surface energy balance algorithms over a corn and soybean production region (Iowa, U.S.) during SMACEX. Agric For Meteorol 149:2082–2097

Elhag M, Psilovikos A, Manakos I, Perakis K (2011) Application of the SEBS water balance model in estimating daily evapotranspiration and evaporative fraction from remote sensing data over the Nile Delta. Water Resour Manag 25:2731–2742

Er-Raki S, Chehbouni A, Hoedjes J, Ezzahar J, Duchemin B, Jacob F (2008) Improvement of FAO-56 method for olive orchards through sequential assimilation of thermal infrared-based estimates of ET. Agric Water Manage 95:309–321

Er-Raki S, Chehbouni A, Boulet G, Williams DG (2010) Using the dual approach of FAO-56 for partitioning ET into soil and plant components for olive orchards in a semi-arid region. Agric Water Manage 97:1769–1778

Eurostat (2011) http://appsso.eurostat.ec.europa.eu/nui/show.do?dataset=ef_lu_pcolive&lang=en

Gavilán P, Lorite IJ, Tornero S, Berengena J (2006) Regional calibration of Hargreaves equation for estimating reference ET in a semiarid environment. Agric Water Manage 81:257–281

Gómez JA, Giráldez JV, Fereres E (2001) Rainfall interception by olive trees in relation to leaf area. Agric Water Manage 49:65–76

Gontia NK, Tiwari KN (2010) Estimation of crop coefficient and evapotranspiration of wheat (Triticum aestivum) in an irrigation command using remote sensing and GIS. Water Resour Manag 24:1399–1414

Hoedjes JCB, Chehbouni A, Jacob F, Ezzahar J, Boulet G (2008) Deriving daily evapotranspiration from remotely sensed instantaneous evaporative fraction over olive orchard in semi-arid Morocco. J Hydrol 354:53–64

Junta de Andalucía. Consejería de Obras Públicas y Transportes (2002) Ortofoto Digital de Andalucía. DVD. ISBN: 84-95083-96-5

Kustas WP, Norman JM (1999) Evaluation of soil and vegetation heat flux predictions using a simple two-source model with radiometric temperature for partial canopy cover. Agric For Meteorol 94:13–29

Lorite IJ, García-Vila M, Carmona MA, Santos C, Soriano MA (2012) Assessment of the Irrigation Advisory Services' recommendations and farmers' irrigation management: a case of study in sourthern Spain. Water Resour Manag 26:2397–2419

Martínez-Cob A, Faci JM (2010) Evapotranspiration of an hedge-pruned olive orchard in a semiarid area of NE Spain. Agric Water Manage 97:410–418

Martín-Vertedor AI, Pérez-Rodríguez JM, Prieto Losada MH, Fereres E (2011) Interactive responses to water deficits and crop load in olive (*Olea europaea L.*, cv. Morisca) II: water use, fruit and oil yield. Agric Water Manage 98:950–958

Michelakis NIC, Vouyoucalou E, Clapaki G (1996) Water use and the soil moisture depletion by olive trees under different irrigation conditions. Agric Water Manage 29:315–325

Minacapilli M, Agnese C, Blanda F, Cammalleri C, Ciraolo G, D'Urso G, Iovino M, Pumo D, Provenzano G, Rayo G (2009) Estimation of actual evapotranspiration of Mediterranean perennial crops by means of remote-sensing based surface energy balance models. Hydrol Earth Syst Sci 13:1061–1074

Norman JM, Kustas WP, Humes KS (1995) Two source approach for estimating soil and vegetation energy fluxes from observations of directional radiometric surface temperature. Agric For Meteorol 77:263–293

Orgaz F, Villalobos F, Testi L, Pastor M, Hidalgo JC, Fereres E (2005) Programación de riegos en plantaciones de olivar. Metodología para el cálculo de las necesidades de agua de riego en el olivar regado por goteo. In: Pastor M (ed) Cultivo del olivo con riego localizado. Junta de Andalucía. Consejería de Agricultura y Pesca, Mundi-Prensa, Madrid, pp 83–137

Palomo MJ, Díaz-Espejo A, Fernández JE, Moreno F, Girón IF (2000) Water balance in an olive orchard. Acta Hort 537:573–580

Perrier A (1982) Land surface processes: vegetation, *in* Eagelson P., ed., Land Surface Processes in Atmospheric General Circulation Models: Cambridge University Press, p. 395–448

Raupach MR (1992) Drag and drag partition on rough surfaces. Boundary-Layer Met 60:375–395

Raupach MR (1994) Simplified expressions for vegetation roughness length and zero plane displacement height as functions of canopy height and area index (Research note). Boundary-Layer Met 71:211–216

Raupach MR (1995) Corrigenda. Boundary-Layer Met 76:303–304

Roerink GJ, Bastiaanssen WGM, Chambouleyron J, Menenti M (1997) Relating crop water consumption to irrigation water supply by remote sensing. Water Resour Manag 11:445–465

Samani Z, Bawazir AS, Bleiweiss M, Skaggs R, Longworth J, Tran VD, Pinon A (2009) Using remote sensing to evaluate the spatial variability of evapotranspiration and crop coefficient in the lower Rio Grande Valley, New Mexico. Irrig Sci 28:93–100

Santos C, Lorite IJ, Tasumi M, Allen RG, Fereres E (2008) Integrating satellite-based evapotranspiration with simulation models for irrigation management at the scheme level. Irrig Sci 26:277–288

Santos C, Lorite IJ, Tasumi M, Allen RG, Fereres E (2010) Performance assessment of an irrigation scheme using indicators determined with remote sensing techniques. Irrig Sci 28:461–477

Tasumi M (2003) Progress in operational estimation of regional evapotranspiration using satellite imagery. Ph. D. Dissertation, University of Idaho, USA, 357pp

Tasumi M, Trezza R, Allen RG, Wright J (2005) Operational aspects of satellite-based energy balance models for irrigated crops in the semi-arid U.S. Irrig Drain Syst 19:355–376

Testi L, Villalobos FJ, Orgaz F (2004) Evapotranspiration of a young irrigated olive orchard in southern Spain. Agric For Meteorol 121:1–18

Villalobos FJ, Orgaz F, Testi L, Fereres E (2000) Measurement and modelling of evapotranspiration of olive (*Olea europaea* L.) orchards. Eur J Agron 13:155–163